HiSST: 2nd International Conference on
High-Speed Vehicle Science Technology
11–15 September 2022, Bruges, Belgium

Hypersonic Shock Tunnel T1: A Parametric Study

Thiago L Assunção[1], Marco A. S. Minucci[1] , Lucas A. G. Ribeiro[1], Pedro. A. S. Matos[1], Vanessa V. Souza[1]

Abstract

This work presents the results of a parametric study carried out at Hypersonic and Aerothermodynamic Laboratory (LAH), employing the Hypersonic Shock Tunnel T1 with a Shock Tube configuration. A computational routine was created using Octave program in order to calculate the flow proprieties under assumption of the calorically perfect gas. Moreover, several Tunnel conditions were analyzed, where 3 experiments (runs) were carried out for each one. Then, the theoretical results were compared to experimental data, such as incident Mach number (M_s) and stagnation pressure (p_5), providing the "loss factor" associated to Tunnel T1 operation. Moreover, still concerning this analysis, it was evaluated the influence of the Driver gas and pressure ratio p_4/p_1 on the flow proprieties, where the results globally agree with literature. Finally, a statistical approach was employed in order to evaluate the repeatability of the results provided by device operation, based on dispersion analysis of the stagnation pressure, where it was possible to notice a low dispersion of the data.

Keywords: *Shock Tunnel, Stagnation Pressure, Parametric Study.*

Nomenclature

Latin
a - speed of the sound
M - Mach number
p - pressure
R – constant of the gases
T - temperature
u – shock wave velocity
Greek
γ – ratio between heat at constant pressure and volume
ρ – density
σ – standard deviation
Subscripts
1 - tunnel driven conditions
4 – tunnel driver conditions
5 – tunnel stagnation conditions
s - incident shock wave conditions
r – reflected shock wave conditions

1. Introduction

Tubes and Shock Tunnels have been widely employed to investigate problems in several fields, such as chemistry, physics, fluid dynamics, structures, etc. Particularly, these devices also have been employed in aerodynamic studies of flows with high velocities and temperatures since 50's. In the middle of 50's, Nagamatsu [1] realized the restrictions imposed by wind tunnels when it was necessary to obtain flows with highs enthalpy and Mach number. As result of these observations, Shock Tunnel was employed to increase the flow velocity up to hypersonic regime through the air passing inside of a nozzle placed at the end of the Shock Tube [2]. Although the short time of the experiments ($\sim ms$) carried out in these pulsed devices, they are able to provide enthalpy levels similar to founded during the atmospheric reentry associated to hypersonic flights. Moreover, it is necessary to stress that the difference between Tunnels and Shock Tubes is that the formers have a convergent-divergent (C-D) nozzle placed at the end of the tube, which is used to generate flows with high Mach numbers in the test section at the nozzle exit, whereas the latter is just sealed at the end by a blind flange.

[1] *Institute for Advanced Studies, São José dos Campos-SP-Brazil, assuncaotla@fab.mil.br*

Concerning the test conditions, several parameters of the Tunnel/Tube operation can be handled as presented by Campbel [3]. In this work the author employed several techniques to obtain large test time, as different gases mixtures in the Driver and different Driver length, for example. Another geometric parameter which can be studied in the test time studies is the Driven length, due to an increase in the amount of gas test and subsequently an increase in test duration. Moreover, Hooker [4] and Polachek & Seeger [5] in their studies about shock waves propagation, realized that the use of an interface gas, for example helium, improve the stagnations conditions. Furthermore, Nascimento [6] presented by his work that employing an extra section with inert gas between the DDS and Driven the stagnation conditions are improved. This section can be named as gaseous piston. Finally, in recent work, Ribeiro *et al.* (not published) presents the influence of the pressure ratio between the Driver and Driven ($p_4/\ p_1$) on the stagnation pressure (p_5). These authors noticed that the stagnation pressure increases as the ratio $p_4/\ p_1$ increase too, as expected by Shock Tube theory [1].

Therefore, this work provides a study about the influence of the operation condition on the several parameters and properties of the Hypersonic Shock Tunnel T1 operating with Tube configuration. Then, time test, stagnation pressure and incident Mach numbers were evaluated for two Driver gases (atmospheric air and helium) and several Driven pressures. Finally, dispersion analysis is employed and from this approach the repeatability results were analyzed.

2. Methods and Facilities

In this part of the work, firstly it will be presented the mathematical modeling employed to analyze theoretically non stationary shock waves propagating in the tunnel. This study is important as it will provide analytical data, under assumption of the calorically perfect gas, without viscous effects and tunnel losses. The second part of this section will present the experimental features of the work, thus the Hypersonic Shock Tunnel T1 is presented, as well as the experimental apparatus and tunnel conditions employed in this study.

2.1. Mathematical Modeling of Tunnel Shock Wave

The mathematical modeling for a shock tube with constant cross section area was employed to estimate the thermodynamic properties in the stagnation region (reservoir conditions) where the equations are presented below. The Mach number of the incident shock wave M_s can be defined as the ratio between shock wave velocity (u_s) and the speed of the sound in the Driven gas (a_1), hence:

$$M_s = \frac{u_s}{a_1} \tag{1}$$

where,

$$a_1 = \sqrt{\gamma_1 R T_1} \tag{2}$$

and γ is equal to ratio between specific heat at constant pressure and volume, respectively ($\gamma = \frac{C_p}{C_v}$), corresponding to 1.4 to atmospheric air. R is the constant of the gases.

To estimate the changes of thermodynamic proprieties across the incident shock wave, it is possible employ the equations below:

$$\frac{\rho_2}{\rho_1} = \frac{(\gamma_1+1){M_s}^2}{(\gamma_1-1){M_s}^2+2} \tag{3}$$

$$\frac{T_2}{T_1} = \frac{2\gamma_1 {M_s}^2-(\gamma_1-1)}{\gamma_1+1}\frac{(\gamma_1-1){M_s}^2+2}{(\gamma_1+1){M_s}^2} \tag{4}$$

$$\frac{p_2}{p_1} = \frac{2\gamma_1 {M_s}^2-(\gamma_1-1)}{\gamma_1+1} \tag{5}$$

where ρ, T e p correspond to density, temperature and pressure, respectively. Moreover, the subscripts "1" and "2" are linked to conditions ahead and behind the incident shock wave, respectively. As noticed in the equations above, the incident Mach number M_s influences on the proprieties after the shock wave

passage, however it is also influenced by any parameters, such as the ratio between the pressure of the Driver (p_4) and Driven (p_1), as well as the gases employed, as can be constated in the equation below:

$$\frac{p_4}{p_1} = \frac{p_2}{p_1}\left\{1 - \left[\frac{a_1(\gamma_4-1)}{a_4(\gamma_1+1)}\right]\left(\frac{{M_s}^2-1}{M_s}\right)\right\}^{-\frac{2\gamma_4}{(\gamma_4-1)}} \tag{6}$$

When the incident shock wave reaches the Driven end, it is reflected and at this moment there is the formation of the stagnation conditions, where the subscript "5" corresponding to proprieties in this region. The reflected Mach number can be obtained by the function:

$$\frac{M_r}{{M_r}^2-1} = \frac{2}{(\gamma_1+1)}\frac{1}{M_2} \tag{7}$$

where, the Mach number behind the incident shock wave (M_2) can be defined as:

$$M_2 = \frac{2({M_s}^2-1)}{\sqrt{[(\gamma_1-1){M_s}^2+2][2\gamma_1{M_s}^2-(\gamma_1-1)]}} \tag{8}$$

From the reflected Mach number M_r , the thermodynamic properties at stagnation region can be obtained employing the equations:

$$\frac{\rho_5}{\rho_2} = \frac{(\gamma_1+1){M_r}^2}{(\gamma_1-1){M_r}^2+2} \tag{9}$$

$$\frac{p_5}{p_2} = \frac{2\gamma_1{M_r}^2-(\gamma_1-1)}{(\gamma_1+1)} \tag{10}$$

$$\frac{T_5}{T_2} = \frac{p_5}{p_2}\frac{\rho_2}{\rho_5} \tag{11}$$

All set of equations presented here was implemented in Octave program and the code was named as Shock_Tube. The results were compared to WiSTL [7], which consists of an online calculator for shock tubes developed in University of Wisconsin-Madison, and presented good agreement, validating the employ of the code in this study. It is necessary to stress that the analytical analysis carried out by the code considers the gases as calorically perfect (γ=cte) and non-viscous effects.

2.2. Facilities and Experimental Setup

The Hypersonic pulsed Shock Tunnel T1 is a device employed to simulate flight conditions by the ground experiments. The sketch of the equipment can be seen in Fig. 1. The Tunnel consists of Driver, DDS (Double Diaphragm Section) and Driven with constant transversal section, except in the final part of the Driven, where there is a circular-to-square transition which respects constant area. Moreover, the test section and dump tank are also part of the device. More details about T1 operation can be consulted in Lima et al. [8].

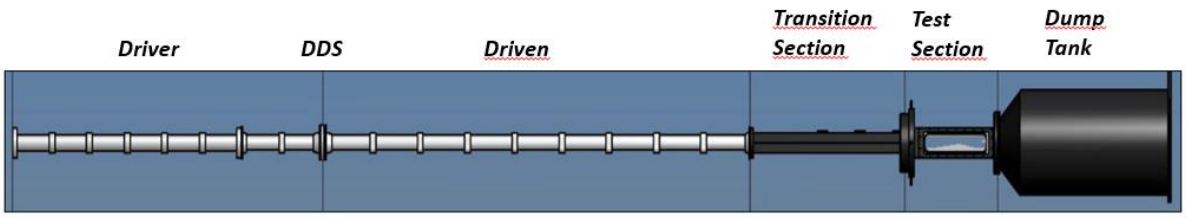

Fig 1. Sketch of Hypersonic Shock Tunnel T1.

It needs to inform that the works carried out in this present study taken into account the Tunnel with a Tube configuration. In other words, there is no passage of the flow through the nozzle, due to the presence of the aluminum diaphragm placed on the transition section end.

The Driver/DDS pressurization was controlled by valves and pressure gauges located at the panel control. The signal generated by the pressure transducers are firstly amplified by a signal conditioner

PCB model 481 and subsequently monitored and saved by Yokogawa oscilloscope DL850E, which can be seen in Fig. 2.

Fig 2. Signal conditioner (left) and oscilloscope (right).

Concerning the pressures transducers, they were of the PCB Piezotronics where the position of each sensor on the Tunnel T1 can be seen in the Fig. 3. The channel used on the oscilloscope, the model, serial number and sensitivity for each sensor used in this study are presented in the Table 1.

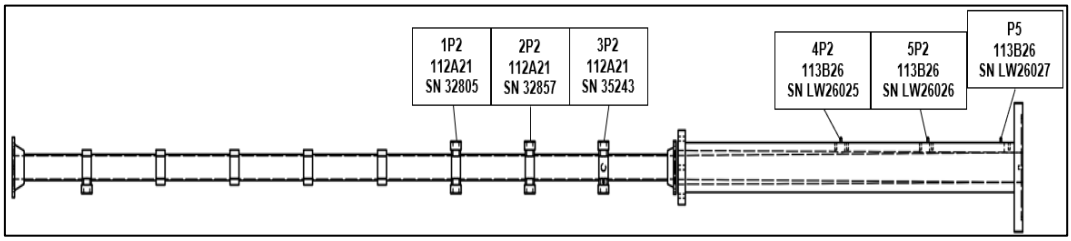

Fig 3. Sensors set up.

Table 1. Sensors information

Channel	*Position*	*Model*	*Serial*	*Sensitivity [mV/kPa]*
CH11	*1P2*	*112A21*	*32805*	*6.2*
CH12	*2P2*	*112A21*	*32857*	*5.87*
CH13	*3P2*	*112A21*	*35243*	*6.94*
CH14	*4P2*	*113B26*	*LW26025*	*1.394*
CH15	*5P2*	*113B26*	*LW26026*	*1.431*
CH16	*P5*	*113B26*	*LW26027*	*1.426*

Regarding the table 1, two sensor models were employed 112A21 and 113B26, where the formers were calibrated and the latter consisted of new devices. The calibration process was carried out following a dynamic calibration approach carried out by Vialta et al. (not published). This method taken into account the entire pressure range of the p_5, analyzing the temporal variations of the sensors, likely providing better accuracy results concerning the associated uncertain. It is necessary to stress that it was the

first time which this process was adopted in the researches at the LAH, where previously the approach based on one-value pressure for calibration was employed [9].

The data were acquired at a frequency of 2 MHz and employing an analysis temporal range of 5 *ms.* This experimental setup provided a sample size of 10,000 points, leading to temporal resolution of 0.5 μs.

Finally, based on the Shock_Tube simulations, a matrix of experiments (Table 2) was determined, where the conditions evaluated in this work can be observed. From this table, it is possible to notice that this work analyzed 6 Tunnel conditions, varying the Driver gas and the ratio between the pressure of the Driver (p_4) and Driven (p_1). Each Tunnel condition was evaluated by 3 tests, providing 18 Tunnel runs. This task had the purpose of evaluate the average values of the parameters and flow proprieties, as well as analyze the Tunnel dispersion features.

Table 2. Matrix of experiments.

Run Number	Driver		DDS		Driven		Ambient Conditions	
	gas	P4 [MPa]	gas	P [MPa]	gas	P1 [kPa]	T[K]	P[kPa)
1, 2 & 3	Helium	4.5	Argon	2.2	Air	96.3	300	96.3
4, 5 & 6	Helium	4.5	Argon	2.2	Air	49	300	96.3
7, 8 & 9	Air	4.5	Argon	2.2	Air	96.3	300	96.3
10, 11 & 12	Air	4.5	Argon	2.2	Air	49	300	96.3
13, 14 & 15	Air	6.0	Argon	3.0	Air	96.3	300	96.3
16, 17 & 18	Helium	6.0	Argon	3.0	Air	96.3	300	96.3

3. Results and Discussions

In this part will be presented the main results of the study, as well as the discussions about these ones. Before analyzing the Tunnel parameters/properties, it is necessary to stress that, at glance, the 3 runs presented reasonable repeatability for each Tunnel condition, except in the case where the Tunnel was operated with p_4*=4.5 Mpa* and p_1*=96.3 kpa.* employing atmospheric air in the Driver. In this specific case, it was noticed a delay in the signals of the 2º run (Fig. 4), possibly associated to trigger sensitivity. Thus, this condition had to be not considered in this work. Moreover, the sensor employed to trigger the system was p_5, where it is analyzed *2.5 ms* before and after this signal rise.

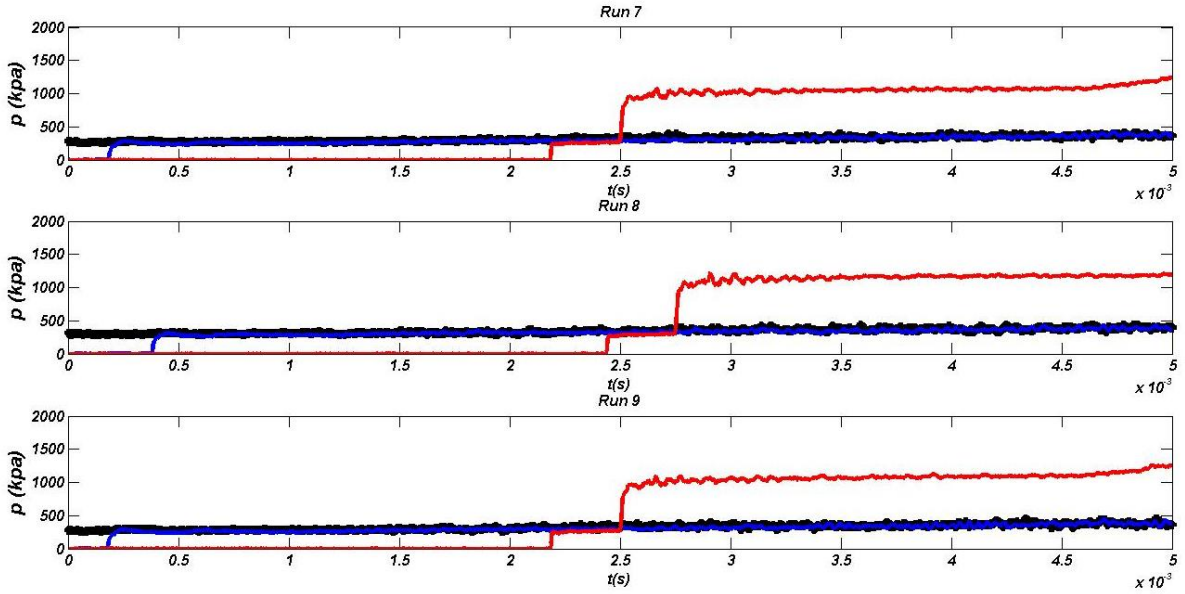

Fig 4. Temporal pressure evolution for p_4=4.5 Mpa and p_1=96.3 kpa, employing atmospheric air in the Driver. Signals: $2p_2$ (black line), $3p_2$ (blue line) e p_5 (red line).

The "step" feature observed in p_5 signal is due to sensor position. In other words, for the fact that not be installed on the blind flange, acquiring only proprieties due to reflected Mach, the sensor is able to acquire p_2 signal too, providing this curious behavior. Finally, the next sections will present the results based on average and dispersion analysis of the 3 runs.

3.1. Mean Results

The results based on the mean analysis of the 3 runs are presented here, where the time test, stagnation pressure p_5, incident Mach number M_S and the losses coefficient are evaluated.

Test Time and $\overline{p_5}$

This part of the work will present the main results of the test time and p_5 which are obtained from the mean values of the 3 runs for each Tunnel condition. Moreover, an average value of this p_5 evaluated at the time test ($\overline{p_5}$) it will be compared to theoretical p_5 obtained by Shock_Tube program. The purpose of this comparison is estimating a loss coefficient (or an empirical efficiency), associated to device operation due to effects not taken into account on the analytical estimation: viscous effects, gas real assumption, diaphragm rupture time, etc.

The approach employed here to determine the test time was consider that, right after the rising of the p_5 signal, a pressure constant value must be considered within 5% of variation. In other words, the instant approximatively 100μs after the rising of p_5 it is considered when the test time starts (t_i), and the final test time (t_f) consists of the instant where p_5 spreads more than 5% of this reference value ($p_5(t_i)$). The test time is obtained by $\Delta t_{Exp}=t_f-t_i$.

This approach had the purpose of avoid initial disturbances associated to reflection of the incident shock wave at the Driven end, although it provides an arbitrary estimation where effectively the measurement of the stagnation pressure begins. The results can be seen in figures below (Figs. 5-9).

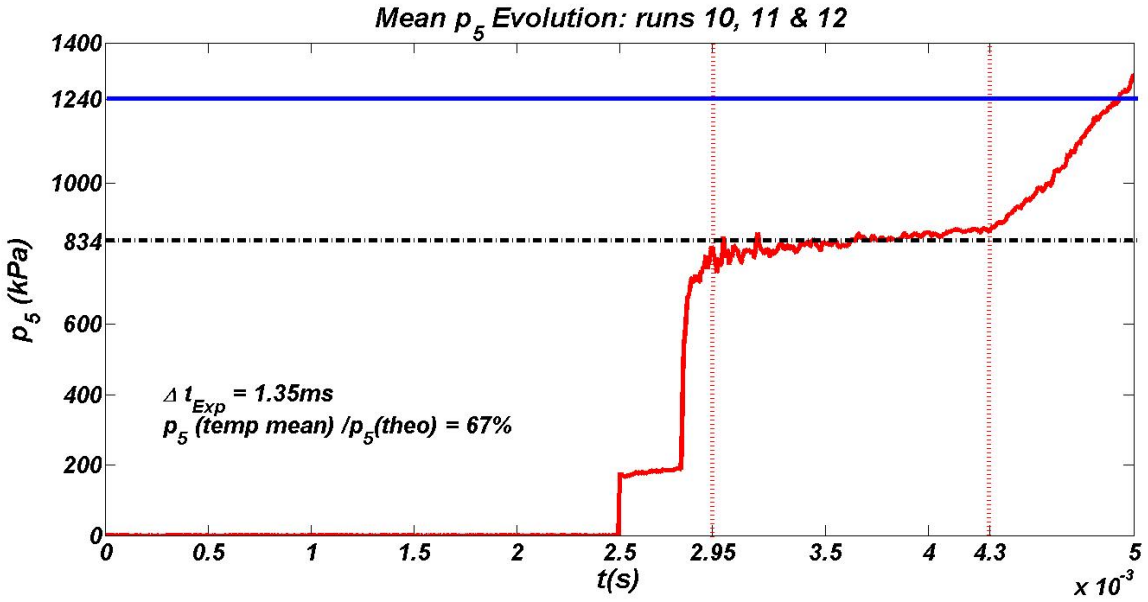

Fig 5. Comparison between p_5 evaluated at the test time ($\overline{p_5}$) (dashed line) x theoretical p_5 obtained by Shock_Tube program (blue line). p_4=4.5 *Mpa* and p_1=49 *kpa*, atmospheric air in the Driver.

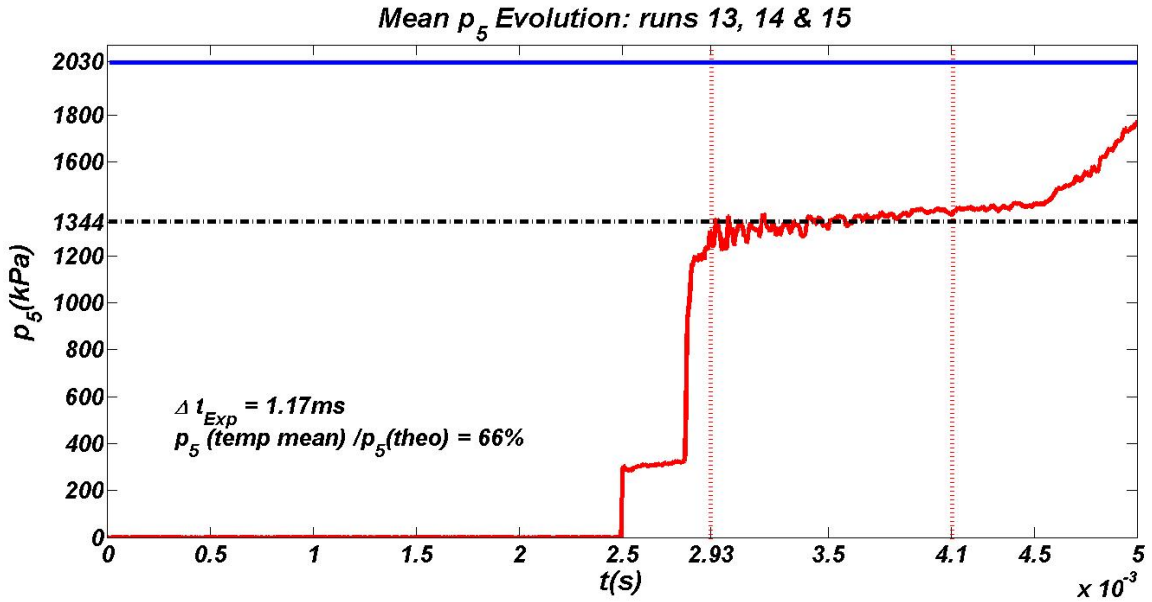

Fig 6. Comparison between p_5 evaluated at the test time ($\overline{p_5}$) (dashed line) x theoretical p_5 obtained by Shock_Tube program (blue line). p_4=6.0 *Mpa* and p_1=96.3 *kpa*, atmospheric air in the Driver.

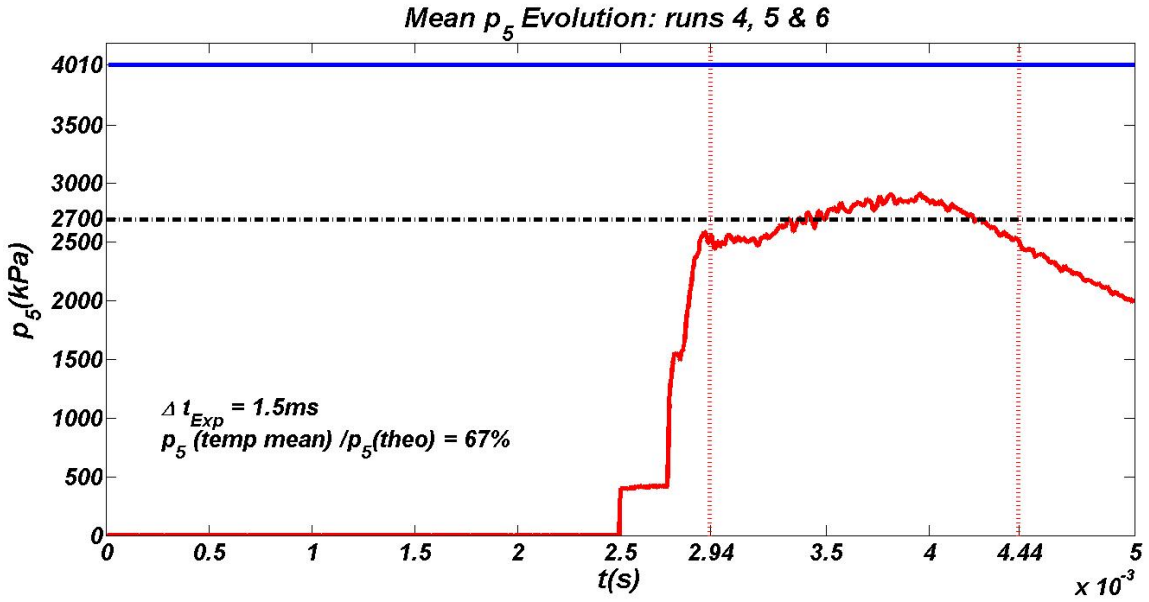

Fig 7. Comparison between p_5 evaluated at the test time ($\overline{p_5}$) (dashed line) x theoretical p_5 obtained by Shock_Tube program (blue line). p_4=4.5 *Mpa* and p_1=49 *kpa*, helium in the Driver.

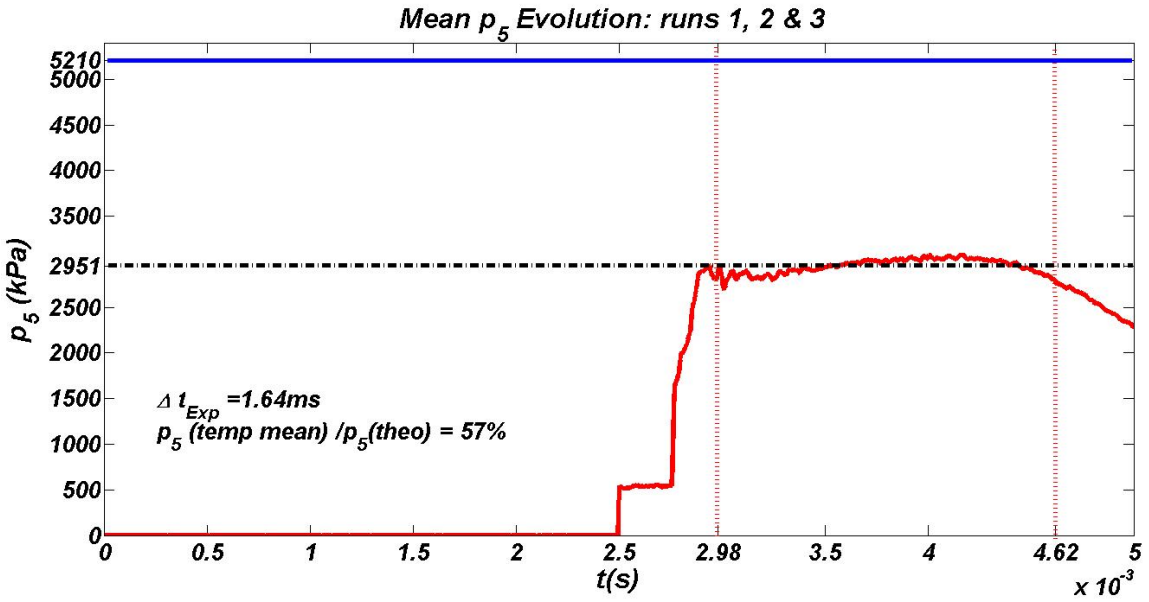

Fig 8. Comparison between p_5 evaluated at the test time ($\overline{p_5}$) (dashed line) x theoretical p_5 obtained by Shock_Tube program (blue line). p_4=4.5 *Mpa* and p_1=96.3 *kpa*, helium in the Driver.

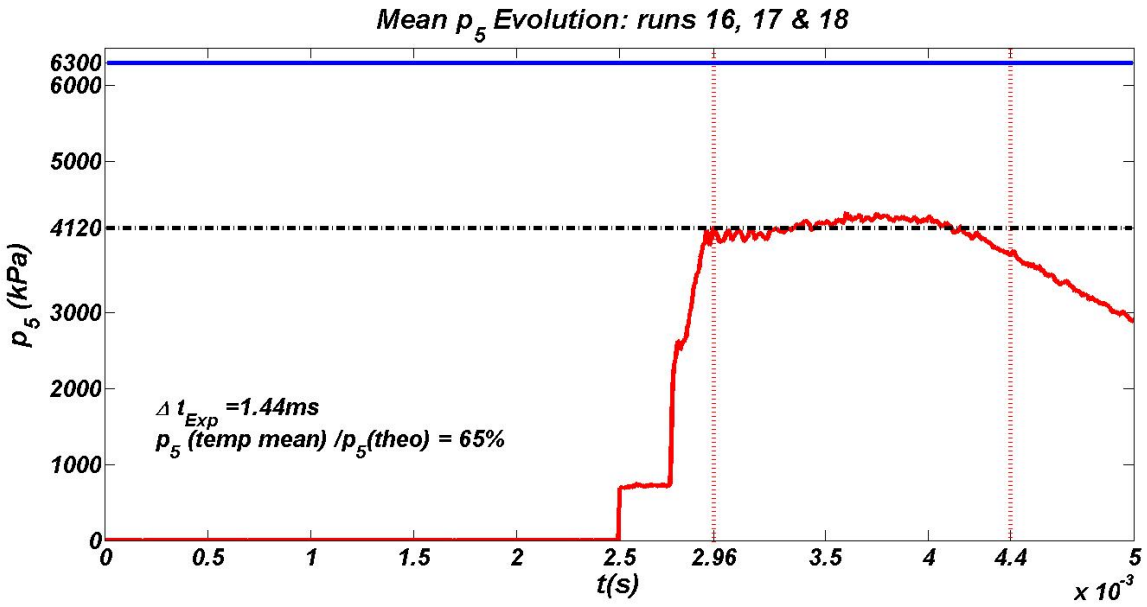

Fig 9. Comparison between p_5 evaluated at the test time ($\overline{p_5}$) (dashed line) x theoretical p_5 obtained by Shock_Tube program (blue line). p_4=6.0 Mpa and p_1=96.3 kpa, helium in the Driver.

Evaluating the figures above, it is possible to notice that employing helium as Driver gas, the time tests are larger than ones employing atmospheric air. It is also possible realize that the high p_5 levels were obtained using helium when compared to experiments carried out with atmospheric air in the Driver. Concerning the p_4/p_1 ratio, the Tunnel condition p_4= 6.0 Mpa / p_1= 96.3kpa provides also the higher levels of p_5 than other conditions, for both gas Driver evaluated. Moreover, analyzing the Table 3 below, it is possible to remark that there is no direct proportionality between p_4/p_1 ratio and the average temporal mean p_5 ($\overline{p_5}$). This results not agree with found by Ribeiro et al. (not published), where the authors observed that p_5 increases as the p_4/p_1 increases too. However, in the present work both pressures varies and not just the Driven one as carried out by the authors. Still analyzing the Table 3, different to absolute $\overline{p_5}$ value, the ratio $\overline{p_5}/p_1$ presents a direct proportionality with p_4/p_1, thus when the latter increases the former increase too.

Table 3. Results comparison

Driver Gas	$p_4\,(Mpa)$	$p_1\,(kpa)$	p_4/p_1	$\overline{p_5}(kpa)$	$\overline{p_5}/p_1$
Air	6.0	96.3	62.3	1344	14
Air	4.5	49.0	91.8	834	17
Helium	4.5	96.3	46.8	2951	30.6
Helium	6.0	96.3	62.3	4120	42.8
Helium	4.5	49.0	91.8	2700	55.1

Taking into account the temporal range of the experiment, another important observation from figures above is that the device operating with helium in the Driver presents a p_5 signal which falls over the time, different to case where the atmospheric air is employed. In this case the signal still increasing

over the time. The possible response for this behavior may be linked to interaction between shock waves, surface contact and expansion waves inside the Tunnel. In other words, perhaps there is interaction between reflect shock wave and expansion ones in the helium case, dropping the stagnation pressure. Otherwise, the interaction which seems be occurring in the atmospheric air case is the interaction between reflect shock waves and surface contact, resulting in the reflected shock from contact surface and increasing the p_5 value. However, future studies taking into account tailored conditions for shock tubes are required for suitable answers for these issues.

Finally, also from the results depicted in Figs. 5-9, it is possible to constate the loss level of the device, obtained by the comparison between the experimental $\overline{p_5}$ value and the theoretical result provided under the ideal gas hypothesis (γ=cte, no viscous effects, diaphragm rupture time negligible). Indeed, globally the results show that the device presents a loss level about 35.6%. This data is able to provide an important parameter to experimental p_5 estimation by the employ of the an adjust coefficient (or empirical efficiency) about 0.64 applied on the theoretical simulation.

M_s: Experimental x Theoretical

The experimental data concerning the incident Mach number (M_S) will be presented and analyzed in this part of the work. The sensors employed for this task, as mentioned in the previous sections, were the *2p2* e *3p2*, which were shown in Fig. 3. Moreover, for incident Mach number obtention, the distance between these sensors (Δx) is important to calculate the shock wave velocity (u_s) and this value can be seen in figure below (Fig. 10).

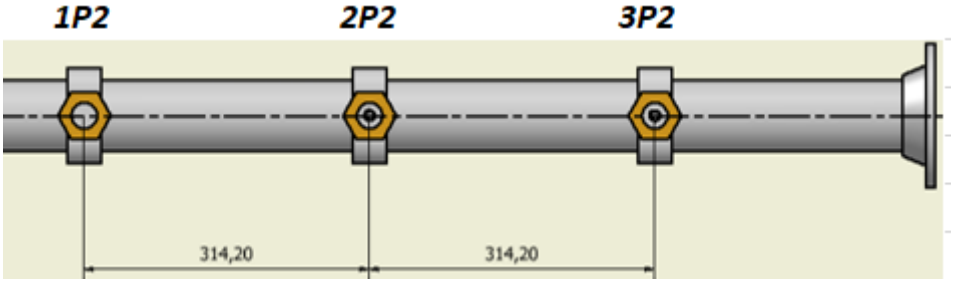

Fig 10. Sensors distance Δx (mm).

Therefore, from the delay of the p_2 signals (time transit) and the displacement of the incident shock wave (Δx), it was able to calculate the shock wave velocity. Furthermore, the information is depicted in Figs. 11-15 and taking into account these data, the experimental incident Mach number ($M_S = u_s / a_1$) was obtained.

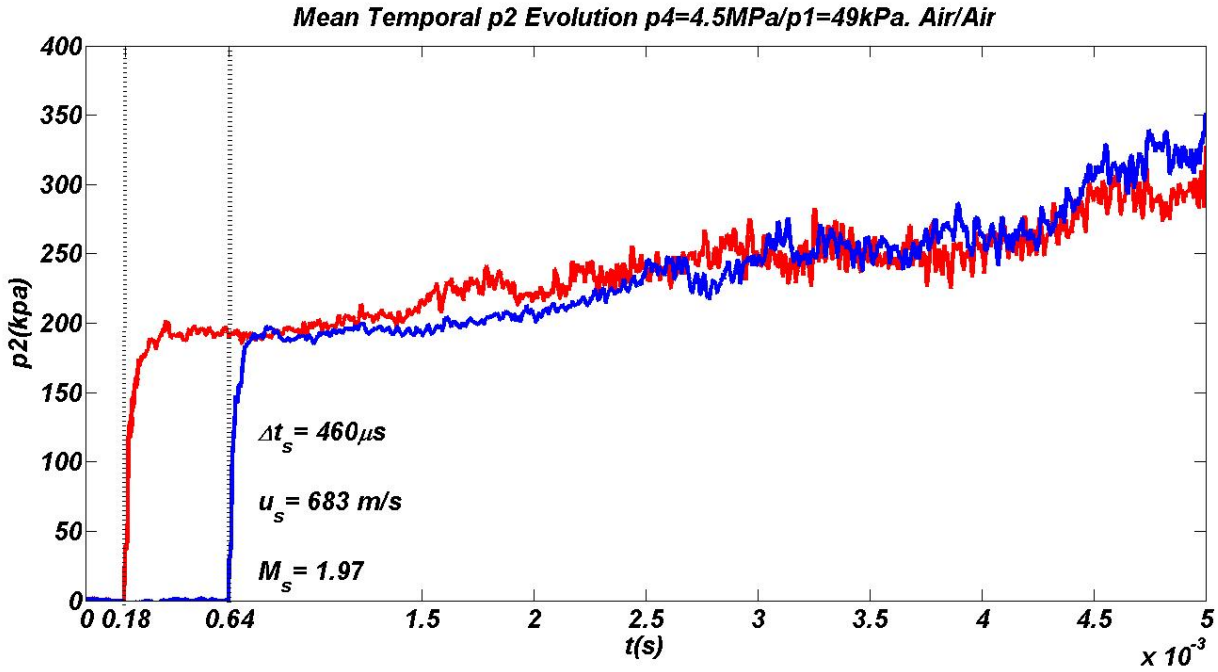

Fig 11. Mean p_2 signal for p_4=4.5 Mpa and p_1=49 kpa, atmospheric air in the Driver. Sensors: $2p_2$ (red) and $3p_2$ (blue).

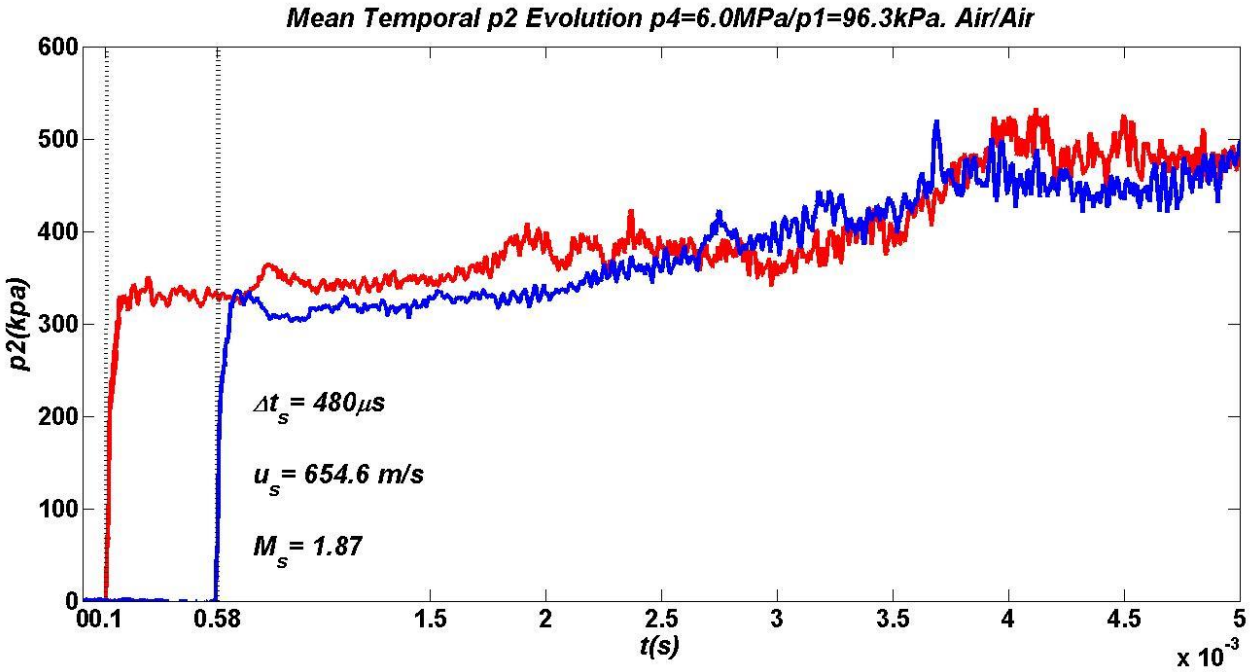

Fig 12. Mean p_2 signal for p_4=6.0 Mpa and p_1=96.3 kpa, atmospheric air in the Driver. Sensors: $2p_2$ (red) and $3p_2$ (blue).

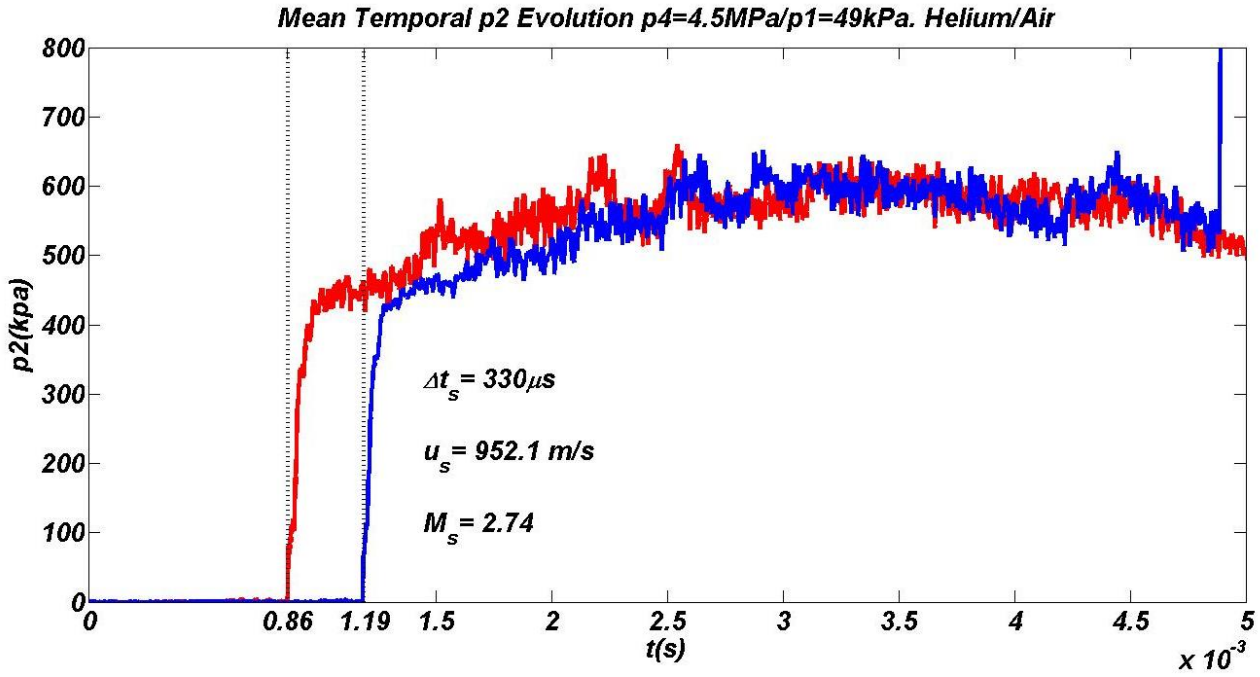

Fig 13. Mean p_2 signal for p_4=4.5 Mpa and p_1=49 kpa, helium in the Driver. Sensors: $2p_2$ (red) and $3p_2$ (blue).

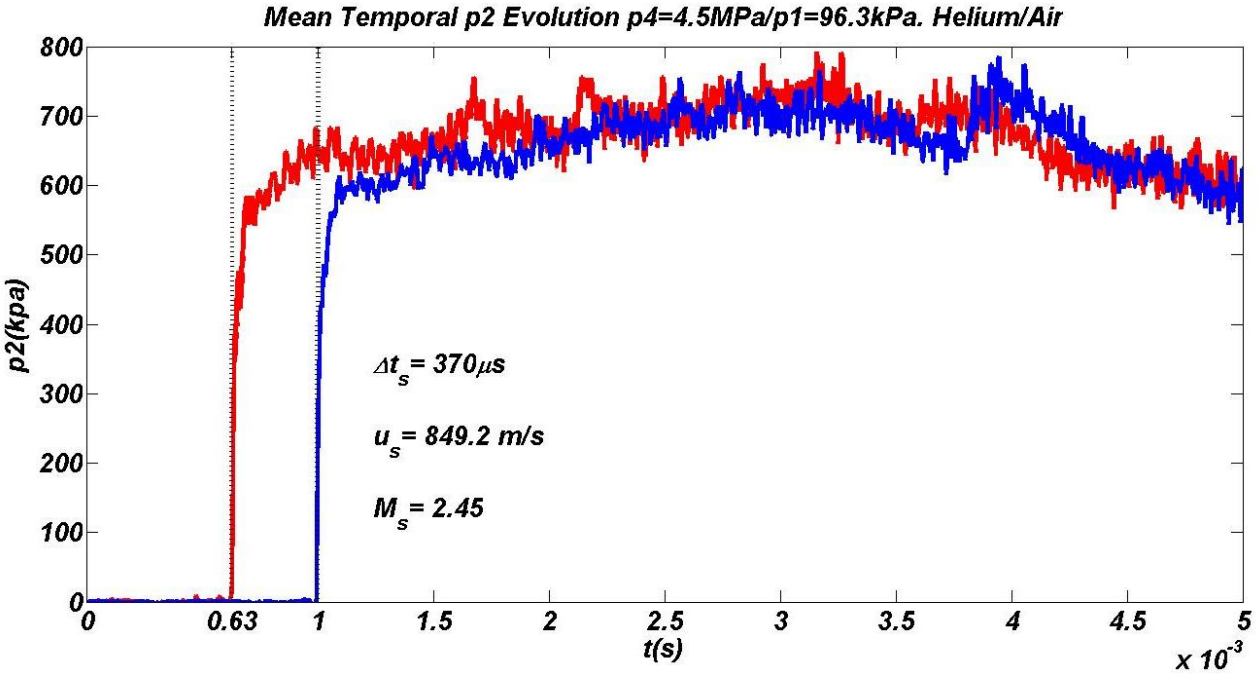

Fig 14. Mean p_2 signal for p_4=4.5 Mpa and p_1=96.3 kpa, helium in the Driver. Sensors: $2p_2$ (red) and $3p_2$ (blue).

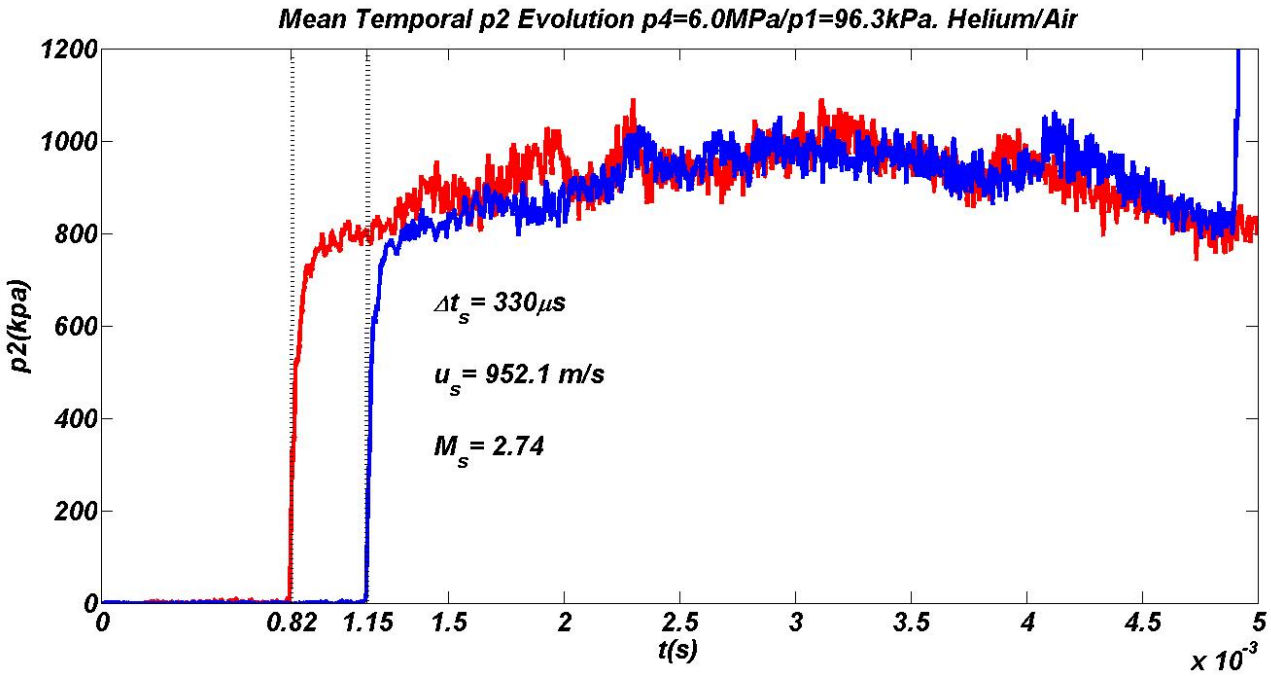

Fig 15. Mean p_2 signal for p_4=6.0 Mpa and p_1=96.3 kpa, helium in the Driver. Sensors: $2p_2$ (red) and $3p_2$ (blue).

The results above shows, as expected, that large incident Mach numbers are reached when inert gas (helium) is employed as Driver gas. This result is also linked to large p_5 values obtained by the use of the same gas. Moreover, different to p_5 results, the incident Mach number globally increases as the ratio p_4/p_1 increases too. The table below (Table 4) presents a comparison between the experimental M_S and the one obtained by Shock_Tube program. In this table, similarly to carried out to p_5 results, an adjust coefficient of about 0.82 can be defined, in order to improve the estimations of the parameter.

Table 4. Incident Mach number comparison.

	M_s experimental x M_s theoretical					
Driver Gas	$p_4\ (Mpa)$	$p_1\ (Kpa)$	p_4/p_1	M_s **theoretical**	M_s **experimental**	Ms_{exp}/Ms_{the}
Air	6.0	96.3	62.3	2.2	1.87	0.85
Air	4.5	49.0	91.8	2.34	1.97	0.84
Helium	4.5	96.3	46.8	3.03	2.45	0.81
Helium	6.0	96.3	62.3	3.25	2.74	0.84
Helium	4.5	49.0	91.8	3.54	2.74	0.77

3.2. Dispersion Results

The results about mean analysis were presented in the previous section. In the present part of the work the main results of a dispersion analysis are treated, considering the 3 runs for each Tunnel condition. It means that the standard deviation (σ) of the p_5 results will be taken into account, providing the fluctuation levels of the stagnation pressure. Then, these values are evaluated at the test time (Δt_{Exp}), leading to a temporal mean value (σ_{mean}) which is compared to mean temporal p_5 ($\overline{p_5}$). The result of this comparison is able to provide an idea about the accuracy of the device. The results can be remarked in the figures below (Figs. 16-20).

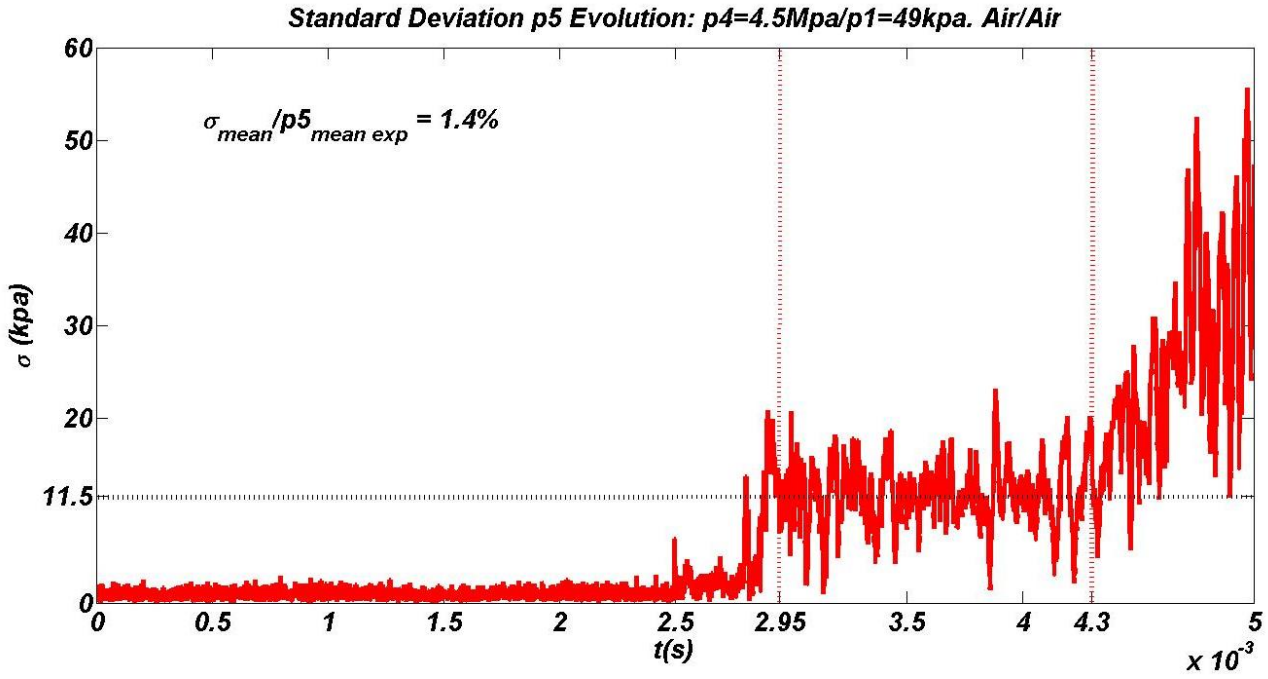

Fig 16. Temporal Evolution of the p_5 Standard Deviation (σ) and comparison between the mean Deviation Standard (σ_{mean}) and $\overline{p_5}$. Tunnel Conditions: p_4=4.5 *Mpa* and p_1=49 *kpa*, atmospheric air in Driver.

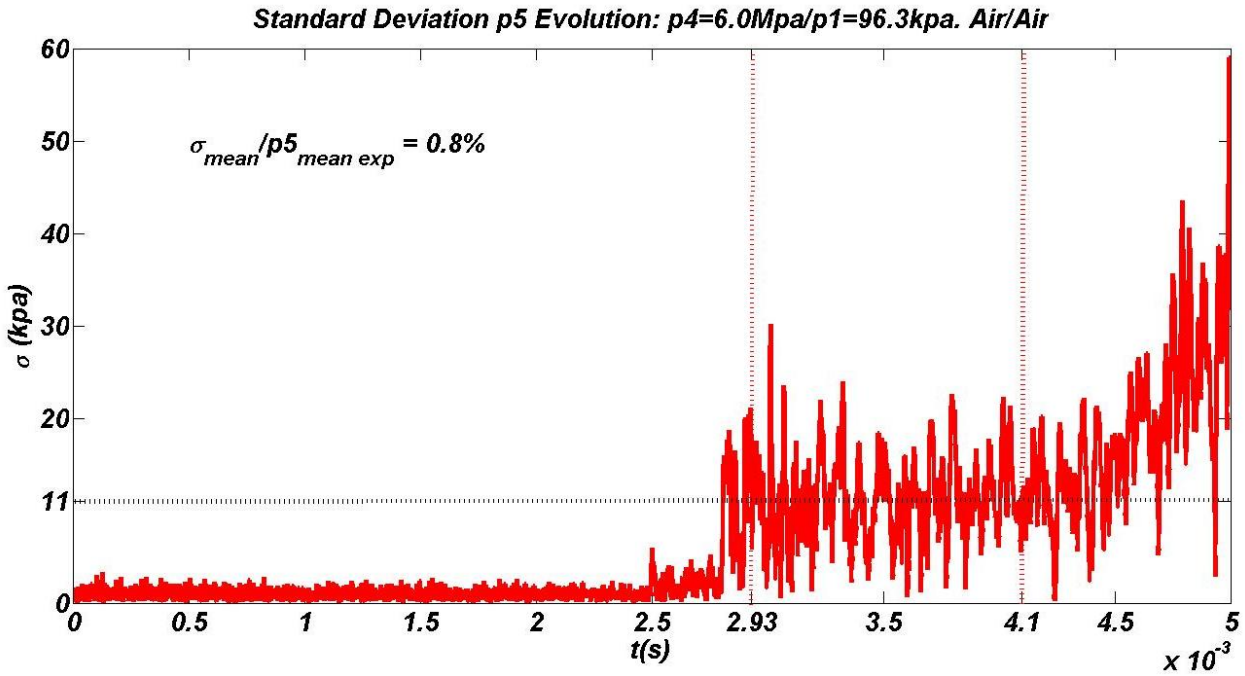

Fig 17. Temporal Evolution of the p_5 Standard Deviation (σ) and comparison between the mean Deviation Standard (σ_{mean}) and $\overline{p_5}$. Tunnel Conditions: p_4=6.0 Mpa and p_1=96.3 kpa, atmospheric air in Driver.

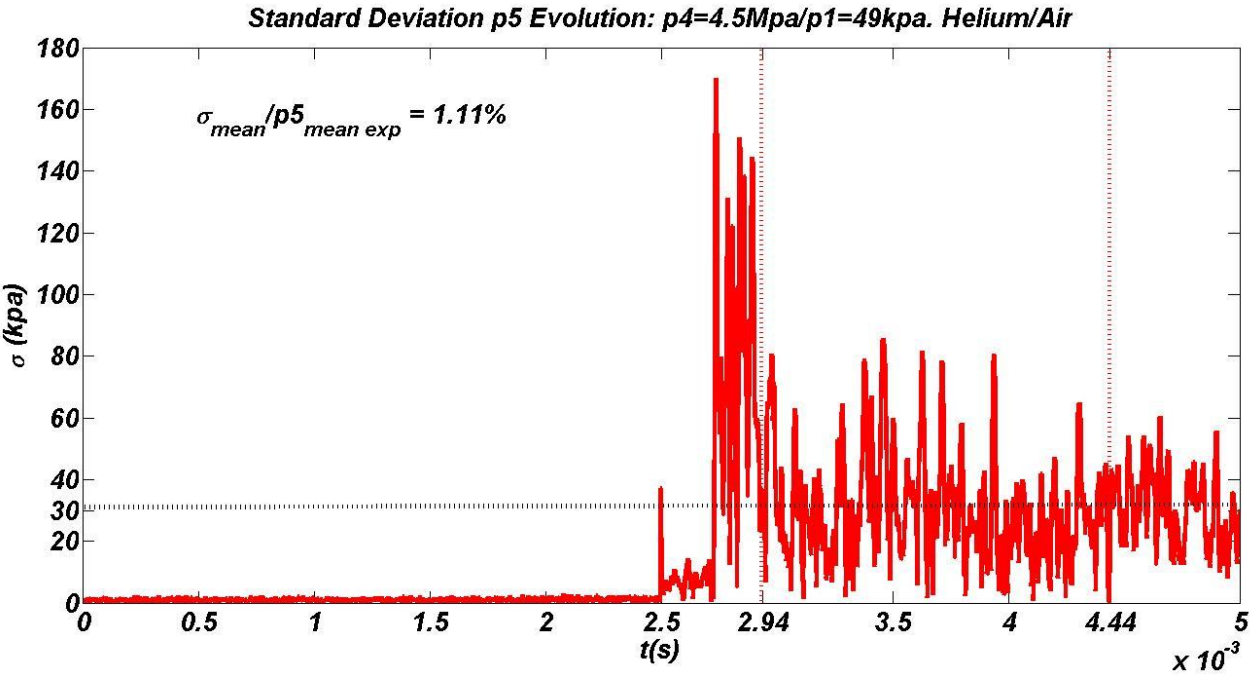

Fig 18. Temporal Evolution of the p_5 Standard Deviation (σ) and comparison between the mean Deviation Standard (σ_{mean}) and $\overline{p_5}$. Tunnel Conditions: p_4=4.5 Mpa and p_1=49 kpa, Helium in Driver.

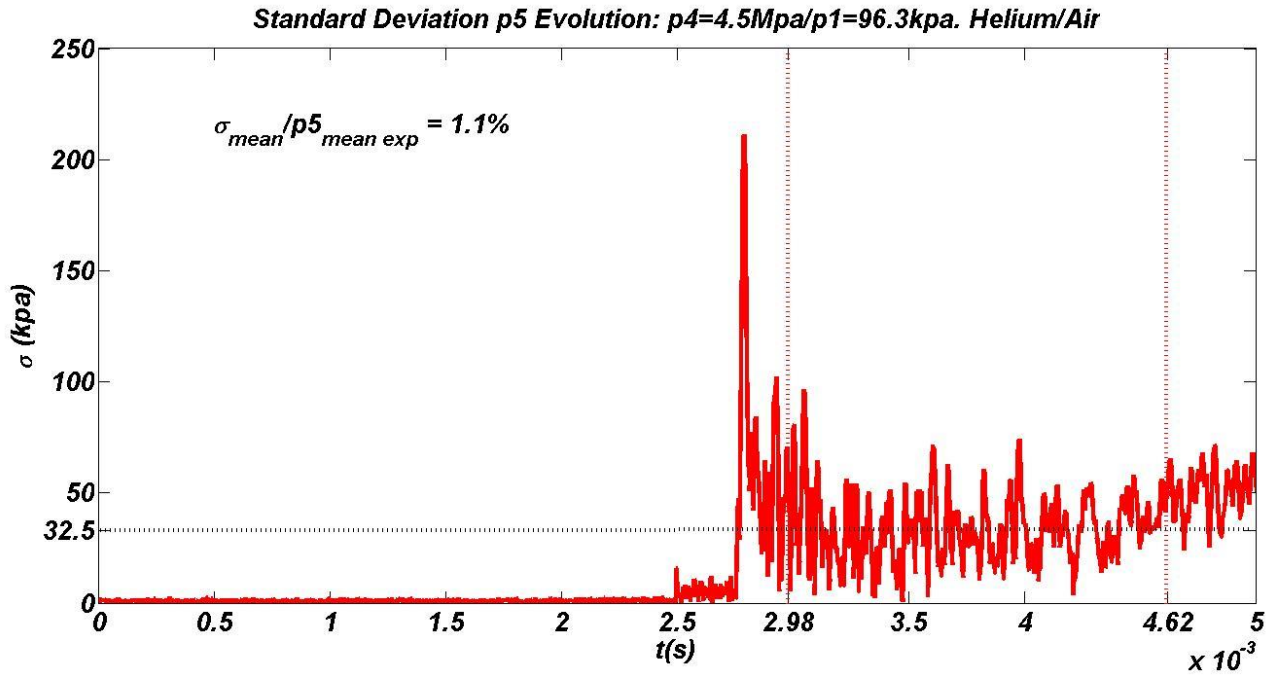

Fig 19. Temporal Evolution of the p_5 Standard Deviation (σ) and comparison between the mean Deviation Standard (σ_{mean}) and $\overline{p_5}$. Tunnel Conditions: p_4=4.5 Mpa and p_1=96.3 kpa, Helium in Driver.

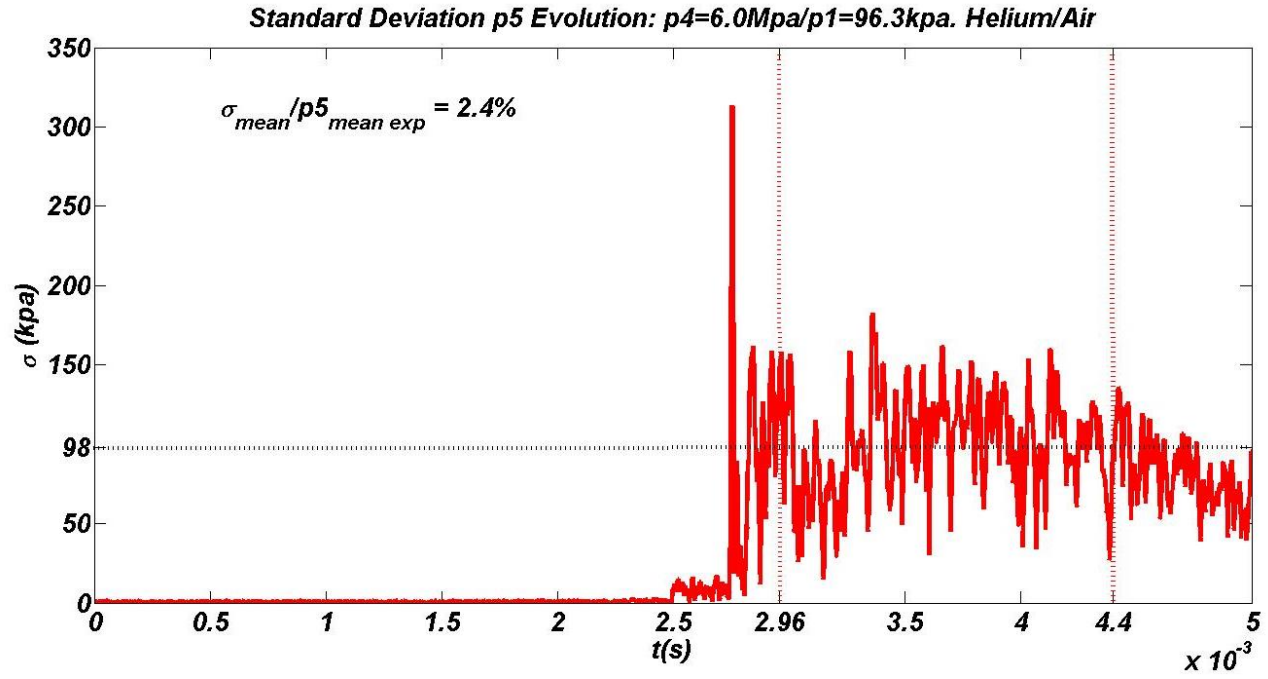

Fig 20. Temporal Evolution of the p_5 Standard Deviation (σ) and comparison between the mean Deviation Standard (σ_{mean}) and $\overline{p_5}$. Tunnel Conditions: p_4=6.0 Mpa and p_1=96.3 kpa, Helium in Driver.

The figures above shows that the largest dispersion in the stagnation pressure ($\sigma_{mean}/\overline{p_5}$) was of 2.4%, observed in the Tunnel condition of *6.0Mpa* in the Driver and *96.3 kpa* in the Driven, operating with helium as gas Driver. This value may be bonded to vibration issues, possibly associated to large Driver pressure. However, in general, these low dispersion values may indicate that the experimental device,

despite of several interference sources (vibration, diaphragm burst time, gas real effects, etc), provides a noticeable repeatability in the stagnation pressure results.

4. Conclusion

This work presented the results of a parametric study carried out at Hypersonic Shock Tunnel T1. A computational routine was created in order to provide the flow proprieties and parameters of the device taking into account the hypothesis of the calorically perfect gas. Moreover, these results for stagnation pressure and incident Mach number were compared to experimental ones, where it was possible to determinate a loss coefficient and consequently an adjust factor/empirical efficiency. The experimental results show that employing helium in the Driver the stagnation pressure increases, agreeing with the literature. Globally, as expected, it was possible observe that the ratio p_4/p_1 also influences on the incident Mach number, increasing this one as the ratio increases too. Finally, carrying out a dispersion analysis on the stagnation pressure results, it was possible to notice the low dispersion of the data, indicating that de device is able to provide experiments with a noticeable repeatability in the results.

References

1. Nagamatsu, H.T.: Shock Tube Technology and Design. Fundamental Data Obtained from Shock-Tube Experiments. New York, 1961.

2. Yoler, Y.A.: Hypersonic Shock Tube. Calif. lnst. of Tech., GALCIT Memo No., 1954.

3. Campbell, M. F., Parise, T., Tulgestke, A. M., Spearrin, R. M., Davidson, D. F., Hanson, R. K.: Strategies for obtaining long constant-pressure test times in shock tubes. Submitted to Shock Waves Journal, 2014.

4. Hooker, W. J.: Testing Time and Contact-Zone Phenomena in Shock-Tube Flows. Physics of Fluids, 1961.

5. Polachek, H., Seeger, R. J.: On Shock-Wave Phenomena; Refraction of Shock Waves at a Gaseous Interface. Physical Review, 1951.

6. Nascimento, M. A. C.: Efeito do Pistão Gasoso em Tubo/Túnel de Choque Quando Operando na Condição de Equilíbrio de Interface. PHD Thesis. Instituto Tecnológico de Aeronáutica (1997)

7. WiSTL Wisconsin Shock Tube Laboratory: <http://silver.neep.wisc.edu/~shock/tools/gdcalc.html>. Accessed 26 may 2020.

8. Lima, B. C., Toro, P. G. P., Santos, A. M.: Analytic Theoretical Analysis of The Incident and The Reflected Shock Waves Applied to Shock Tubes. International Congress Of Mechanical Engineering (COBEM 2013), 4, 2013, Brazil.

9. Damião, A. A., Toro, P. G. P., Sala Minucci, M. A., Cordeiro Marcos, T. V., Romanelli Pinto, D., Mantovani, A. F.: Calibration Methodology for Piezoelectric Pressure Transducers Using Supersonic Shock Tubes. 13rd Brazilian Congress of Thermal Sciences and Engineering, 2010, Brazil

